



## Original Research Paper

## Improving hydrothermal performance of hybrid nanofluid in double tube heat exchanger using tapered wire coil turbulator

Sumit Kr. Singh, Jahar Sarkar\*

Department of Mechanical Engineering, Indian Institute of Technology (B.H.U.), Varanasi, UP 221005, India



## ARTICLE INFO

## Article history:

Received 7 December 2019  
 Received in revised form 19 February 2020  
 Accepted 3 March 2020  
 Available online 13 March 2020

## Keywords:

Double-tube heat exchanger  
 Tapered wire coil  
 Hybrid nanofluid  
 Thermal performance factor  
 Pressure drop  
 Entropy generation

## ABSTRACT

Tapered wire coil insert is proposed as a novel enhancer in the double tube heat exchanger and experimental studies on  $\text{Al}_2\text{O}_3 + \text{MgO}$  hybrid nanofluid flowing under the turbulent condition are performed to investigate the hydrothermal characteristics. Effects of using tapered wire coil turbulator and hybrid nanofluid on the hydrothermal behaviors are examined for different coil configurations (Converging (C) type, Diverging (D) type and Converging-Diverging (C-D) type) and hybrid nanofluid inlet temperatures and volume flow rates. Results show that D-type wire coil insert promotes better hydrothermal performance as compared to C-type and C-D type. Nusselt number and friction factor of hybrid nanofluid using D-type, C-D type and C-type wire coil inserts enhance up to 84%, 71% and 47%, and 68%, 57% and 46%, respectively than that of water in tube without insert. The entropy generation of hybrid nanofluid is lower than that of base fluid in all cases. The thermal performance factor for hybrid nanofluid is found more than one with all inserts. The thermal performance factor is observed a maximum of 1.69 for D-type coil. The study reveals that the hybrid nanofluid and tapered wire coil combination is promising option for improving the hydrothermal characteristics of double pipe heat exchanger.

© 2020 The Society of Powder Technology Japan. Published by Elsevier B.V. and The Society of Powder Technology Japan. All rights reserved.

## 1. Introduction

Many active and passive heat transfer augmentation techniques have been established for the heat exchanger. In the active method, the heat transfer rate is enhanced by adding external power sources such as rotating the surface, impinging jets, fluid vibration, etc. On the other hand, the passive method does not require any power sources, easy to handle and low-cost implementation. That's why, recently, the passive technique has become a promising method. Among the passive techniques, the turbulator is extensively used in the heat exchanger. However, most of the researchers investigated the thermal characteristics of heat exchanger using twisted tape or wire coil inserts [1–5]. Both the tube inserts are generally more active in the laminar flow regime as compared to turbulent flow. Twisted tape insertion is beneficial than wire coil insert without considering pressure drop penalty; however, the wire coil inserts yield better overall performance by considering

the pressure drop penalty [6–7]. Wire coil insertions as turbulator have been used to increase the hydrothermal characteristics by diminishing the boundary layer thickness and thus increasing the turbulent flow intensity. High turbulent flow intensity can improve the hydrothermal characteristics by reducing the stream cross-section area, increasing the temperature gradient and flow velocity with a penalty of pressure drop. Within the last decade, several experiments were carried out to find out the influence of wire coil inserts on the heat transfer and friction factor characteristics of water for various heat exchangers [8–11].

Recently, the mono or hybrid nanofluids (referred to the composition of one or more variants type of nanoparticles dispersed in base fluid) have been appeared as an advanced heat transfer fluid due to significant improvement of heat transfer characteristics [12–15]. Hence, the combination of helical coil inserts and nanofluid together may lead to an increase in the hydrothermal characteristics of the heat exchanger significantly and many investigations have been conducted in the last few years [16]. Chandrasekar et al. [17–18] conducted an experiment to study the water-based alumina nanofluid heat transfer and pressure drop in the tube with coil inserts and found enhancement due to the effect of dispersion or back-mixing. Saeedinia et al. [19]

Abbreviations: C, convergence; C-D, convergence-divergence; D, divergence; TPF, thermal performance factor; TEM, transmission electron microscope; lpm, liter per minute.

\* Corresponding author.

E-mail address: [jsarkar.mec@itbhu.ac.in](mailto:jsarkar.mec@itbhu.ac.in) (J. Sarkar).



**Table 1**  
Thermo-physical properties of base fluid, nanoparticles and hybrid nanofluid.

Materials	Thermal conductivity (W/m.K)	Density (kg/m <sup>3</sup> )	Specific heat capacity (J/kg.K)	Viscosity (Pa.s)
Water	0.6014	995	4183	0.0007623
Al <sub>2</sub> O <sub>3</sub>	40	3900	880	–
MgO	48.4	3580	877	–
Al <sub>2</sub> O <sub>3</sub> + MgO (Hybrid nanofluid)	0.6047	1000.1	4171	0.0008187

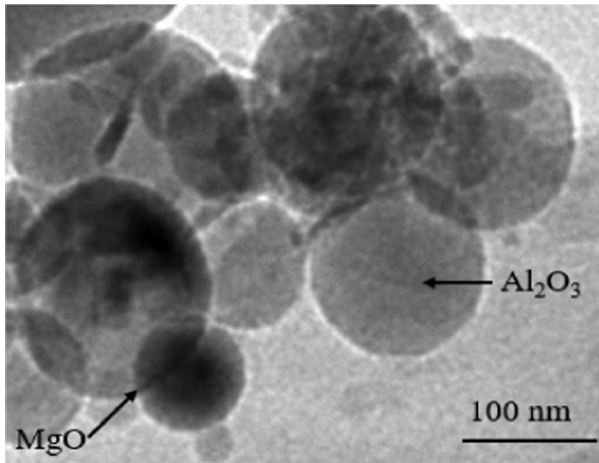


**Fig. 1.** TEM image of Al<sub>2</sub>O<sub>3</sub> + MgO hybrid nanofluid.

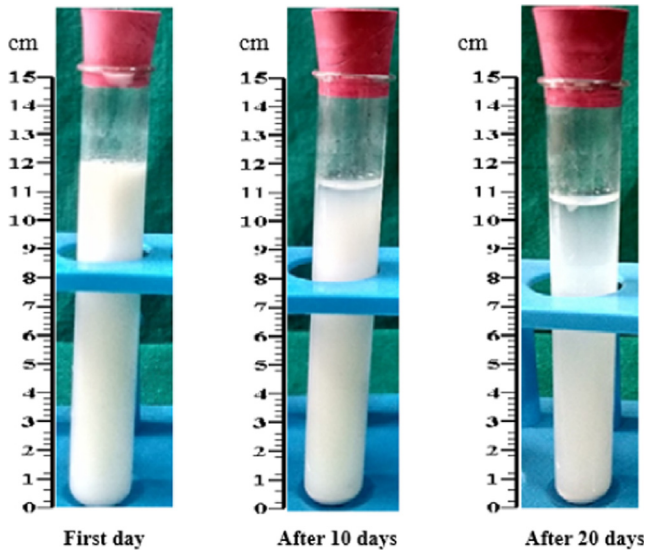


**Fig. 2.** Sedimentation observation of Al<sub>2</sub>O<sub>3</sub> + MgO (0.1 vol.%) hybrid nanofluid.

fluid) is fed through the inner tube and cold fluid (water) is passed through annulus in the opposite direction. The inner tube has internal and external diameters of 18 and 26 mm, respectively, whereas the annulus has an internal diameter of 42 mm. To decrease the heat losses to the surrounding, the outer tube was wrapped with asbestos rope. The temperatures of both fluids were determined by using PT-100 thermocouples. Calibration of all the thermocouples was done with a portable calibrator before fixing them. Two rotameters (one is float type and other is turbine type) were installed with control valves in each circular loop to determine the flow rates of the fluids. Float type rotameter was implemented in the hot fluid loop whereas turbine type rotameter was in the cold fluid loop. The control valves were implemented to

regulate the flow rate of both fluids. Pressure drop through the inner tube and outer tube were measured by U-tube manometers. In the experiment, the temperature of the water was kept at 30 °C and maintained a uniform flow rate of 25 lpm. The hot fluid flowed through the inner pipe at a constant temperature of 50 °C, 60 °C and 70 °C with a volumetric flow rate ranging from 4.2 lpm to 15 lpm. In each test run, all the temperatures and pressure drops were recorded at a period of 15–20 min to ensure the steady-state. The specifications of the concentric tube heat exchanger and geometries of tapered wire coils and operating conditions are summarized in Table 2.

The pictorial view of tapered wire coil with different configurations namely convergence type wire coil (C-type), divergence type wire coil (D-type) and convergence-divergence type wire coil (C-D type) as shown in Fig. 4. The tapered wire coil is made of aluminium with 13 mm diameter (D) from one end and 6.5 mm diameter ( $d = D/2$ ) from another end with a constant pitch of 10 mm. All the dimensions of the wire coil were measured by using Vernier caliper with the least count of 0.02 mm.

### 2.3. Data reduction

The heat transfer rate from hot hybrid nanofluid and cold fluid have been calculated by,

$$Q_{hnf} = \dot{m}_{hnf} c_{p,hnf} (T_{h,in} - T_{h,out}) \quad (1)$$

$$Q_w = \dot{m}_w c_{p,w} (T_{w,out} - T_{w,in}) \quad (2)$$

The average heat transfer rate can be expressed as,

$$Q_v = (Q_{hnf} + Q_w) / 2 \quad (3)$$

The overall heat transfer coefficient (inner tube side) is expressed by,

$$U_i = \frac{Q_v}{A_i \times \Delta T_{LMTD}}, \Delta T_{LMTD} = \frac{(T_{h,in} - T_{w,out}) - (T_{h,out} - T_{w,in})}{\ln \left( \frac{T_{h,in} - T_{w,out}}{T_{h,out} - T_{w,in}} \right)} \quad (4)$$

The inner tube side (hybrid nanofluid) heat transfer coefficient can be evaluated by the equation without considering fouling,

$$\frac{1}{U_i A_i} = \frac{1}{h_i A_i} + \frac{\ln \left( \frac{d_o}{d_i} \right)}{2\pi k L} + \frac{1}{h_o A_o} \quad (5)$$

Where, the cold fluid side heat transfer coefficient is measured by Gnielinski's equation,

$$Nu_o = \frac{\left( \frac{f}{8} \right) (Re - 1000) Pr}{1 + 12.7 \left( \frac{f}{8} \right)^{(1/2)} (Pr^{(2/3)} - 1)} \quad (6)$$

where, the friction factor is determined by Petukhov correlation,

$$f = (0.79 \ln(Re) - 1.64)^{-2}; 2300 < Re < 10^6; 0.5 < Pr < 2000 \quad (7)$$

The value of  $Nu_o$  from the Eq. (6) is substituted in Eq. (8) to evaluate the cold fluid side heat transfer coefficient.

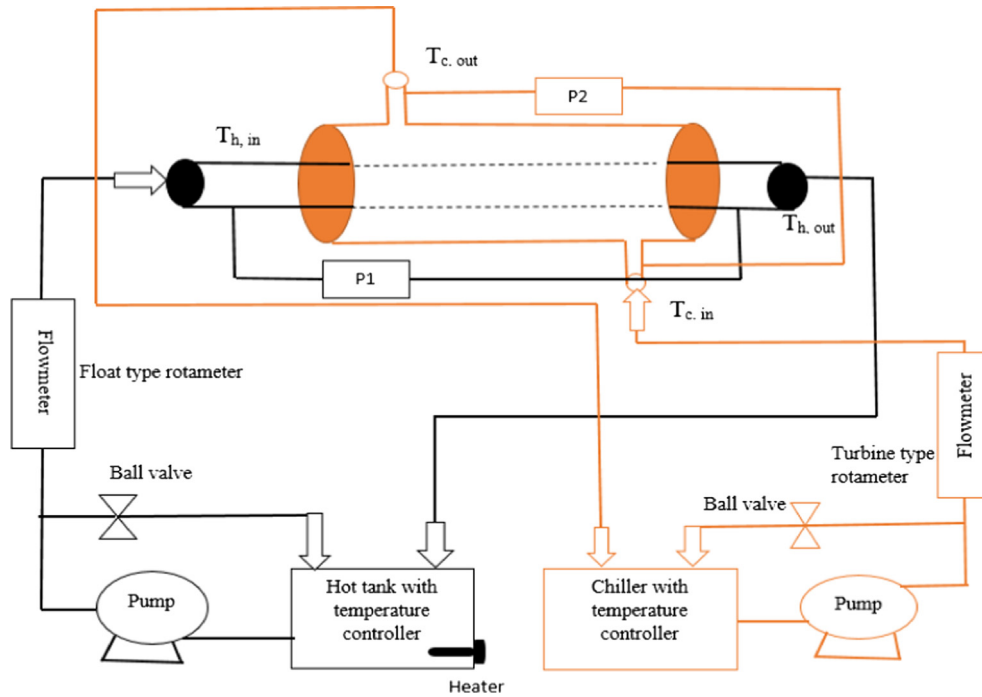


Fig. 3. Schematic diagram of the experimental setup.

Table 2

Details of experimental setup and operating conditions.

Parameter	Value
Inner tube internal diameter	18 mm
Inner tube external diameter	26 mm
Length of the tube	570 mm
Outer tube internal diameter	42 mm
Wire thickness	2 mm
Pitch of the tapered wire coil, P	10 mm
Larger end diameter of tapered wire coil, D	13 mm
Smaller end diameter of tapered wire coil, d	6.5 mm
Nanofluid Reynolds number	9000 to 40000
Nanofluid inlet temperature	50 °C, 60 °C and 70 °C

$$h_o = \frac{Nu_o \times k_o}{d_e} \quad (8)$$

where  $d_e$  is the equivalent diameter of the annulus fluid and given by,

$$d_e = \left( d_{ot,i}^2 - d_{it,o}^2 \right) / d_{it,o} \quad (9)$$

Then the hot fluid side (hybrid nanofluid) heat transfer coefficient has been evaluated by using Eqs. (5)–(8). The Nusselt number of hybrid nanofluid has been estimated by,

$$Nu_{hnf} = h_{hnf} d_{it,i} / k_{hnf} \quad (10)$$

The friction factor is given by,

$$f = \frac{\pi^2}{8} \Delta p \left( \frac{\rho_{hnf} d_{it,i}^2}{\dot{m}_{hnf}^2 L} \right) \quad (11)$$

The thermal performance factor (TPF) is the ratio of effective change in Nusselt number to change in friction factor. It is a vital parameter that indicates the potential of tapered wire coil for practical applications.

$$TPF = \left( \frac{Nu_{hnf}}{Nu_{bf}} \right) / (f_{hnf} / f_{bf})^{(1/3)} \quad (12)$$

For each side of the double tube heat exchanger, the total entropy generation is expressed as,

$$S_{gen,tot} = S_{gen,ht} + S_{gen,f} \quad (13)$$

The entropy generation due to heat transfer ( $S_{gen,ht}$ ) can be expressed as follow;

$$S_{gen,ht} = \dot{m}_{hnf} c_{p,hnf} \ln \left( \frac{T_{h,out}}{T_{h,in}} \right) + \dot{m}_c c_{p,c} \ln \left( \frac{T_{c,out}}{T_{c,in}} \right) \quad (14)$$

The entropy generation due to pressure drop ( $S_{gen,f}$ ) can be expressed as follow;

$$S_{gen,f} = \frac{\dot{m}_{hnf} \times \Delta p_h}{\rho_h \times T_{avg,h}} + \frac{\dot{m}_c \times \Delta p_c}{\rho_c \times T_{avg,c}} \quad (15)$$

#### 2.4. Uncertainty analysis

Table 3 presents the uncertainty of measuring apparatuses used in the experiment. Based on these uncertainties, the maximum uncertainties of the predicted parameters such as Reynolds number, Nusselt number, friction factor, TPF and entropy generation have been calculated and are also depicted in Table 3.

#### 2.5. Validation of plain tube with water

The experiments were performed with water in a plain tube to validate the experimental data. The hot water at 60 °C and cold water at 30 °C were supplied. At steady-state, all the parameters such as temperatures and pressure drop of hot and cold fluid were noted at the Reynolds number from 9000 to 40,000 and used for determining the Nusselt number. The experimentally obtained Nusselt number was validated with Gnielinski's correlation as seen in Fig. 5. The results indicate that the experimentally results data reasonably agreed with the correlation and showed a maximum deviation of 7.5%.

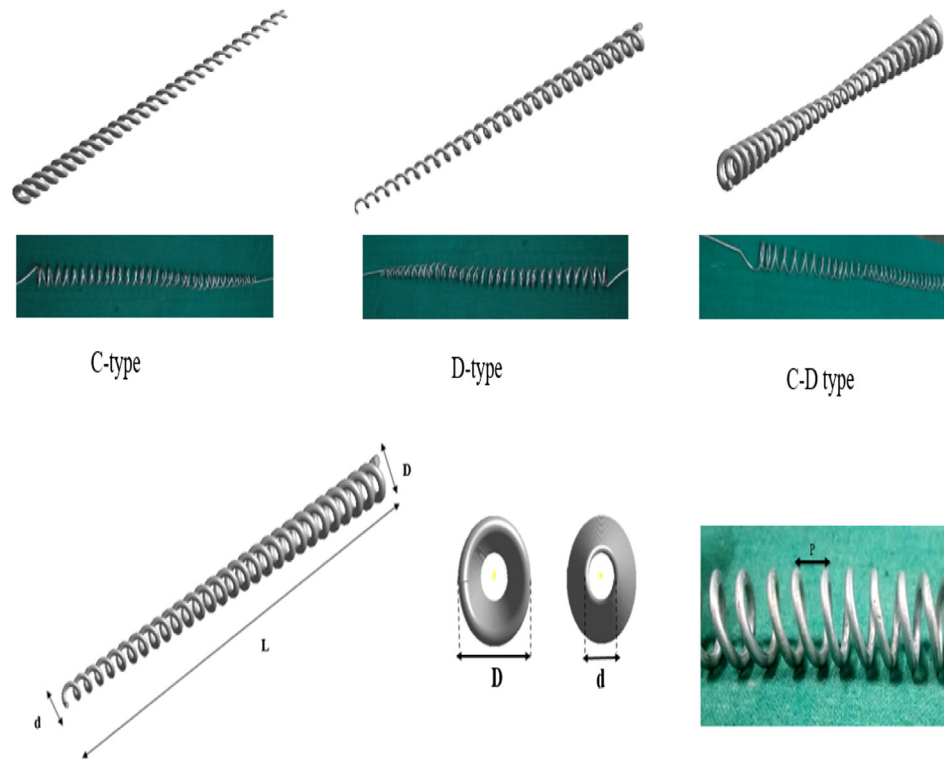


Fig. 4. Tapered wire coil with different configurations and dimensions.

Table 3  
Measuring apparatus accuracy and uncertainty of parameters.

Parameter	Accuracy
Temperature (0–750 °C)	±0.2 °C
Mass flow rate (0–2 kg/s)	±0.003 kg/s
Density (kg/m <sup>3</sup> )	±1%
Viscosity (Pa·s)	±1%
Thermal conductivity (W/m·K)	±1%
Pressure drop (0–30 mm Hg)	±3.02%
Reynolds number	±1.56%
Heat transfer coefficient	±3.73%
Nusselt number	±3.86%
Friction factor	±4.45%
TPF	±5.84%
Entropy generation	±3.57%

### 3. Results and discussion

#### 3.1. Nusselt number and friction factor

Figs. 6 and 7 show the influence of using tapered wire coil on the Nusselt number and friction factor of hybrid nanofluid with different coil configurations (C-type, D-type and C-D type) at an inlet temperature of 60 °C. The results indicate that while increasing Reynolds number, Nusselt number increases and friction factor drops due to a decrease of both hydrodynamic and thermal boundary layer thickness. Tapered wire coil insertions provide better hydrothermal characteristics by diminishing the boundary layer thickness and thus increasing the turbulent flow intensity at different radial distances in the tube. The Nusselt number of hybrid nanofluid is greater than that of the base fluid (water). It is due to the increase of thermal conductivity of nanoparticles and increase of fluid viscosity which causes to be lost the fluid movement which promotes better heat transfer. Also, the results reveal that D-type wire coil promotes enhanced heat transfer than that of the C-type and C-D type because it provides higher contact surface

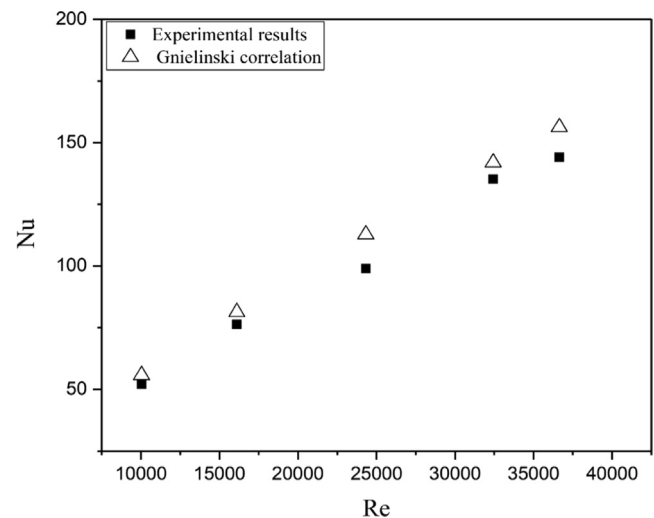
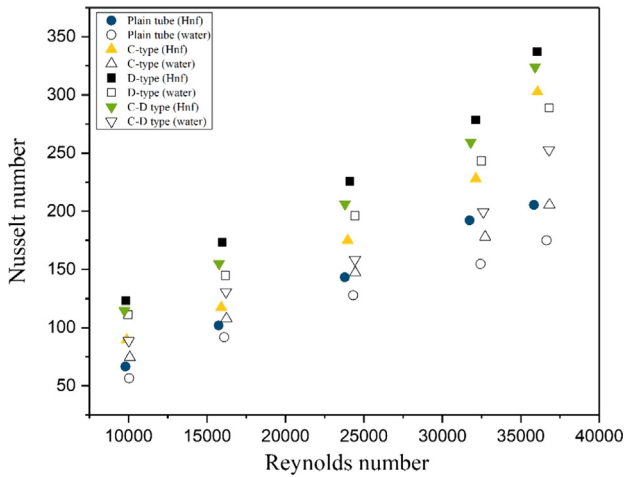
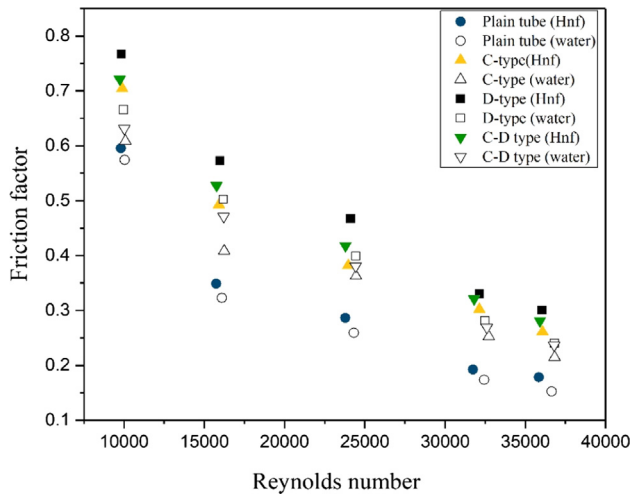


Fig. 5. Validation of Nusselt number with Reynolds number for water in a plain tube.

area between fluid and wall surface when the fluid decelerates from D-type wire coil. In Fig. 7, it is found that using tapered wire coil results in an increase of friction factor above that of plain wire coil as the fluid contact with the surface area of wire coil is greater due to longer path flow which leads to higher friction loss. D-type wire coil shows a higher friction factor than that of the C-type and C-D type because the flow is disturbed at the entry of D-type wire coil turbulator and yields a higher pressure drop across the length of the tube. The average Nusselt number and friction factor of 0.1% hybrid nanofluid flowing in the inner tube with D-type, C-D type and C-type wire coil insertions respectively, enhance 1.64 to 1.84, 1.57 to 1.71, 1.34 to 1.47 times and 1.28 to 1.68, 1.21 to 1.57 and 1.18 to 1.46 times, respectively, than that for the smooth tube with water (base fluid).



**Fig. 6.** Variation of Nusselt number with Reynolds number for different coil configurations.



**Fig. 7.** Variation of friction factor with Reynolds number for different coil configurations.

The variations of Nusselt number and friction factor of hybrid nanofluid for different configurations with different inlet temperatures of 50 °C, 60 °C and 70 °C at a volume flow rate of 10 lpm are illustrated in **Figs. 8 and 9**. The results show that the Nusselt number increases and friction factor decreases with increasing the inlet temperature of hybrid nanofluid. The Nusselt number rises with an increase in temperature because of the augmentation in thermo-physical properties of the hybrid nanofluid such as viscosity, density and thermal diffusivity. At the same instant, the pressure drop in the pipe also falls with the rise in inlet temperature as the fluid viscosity decreases with an increase in inlet temperature. Using a D-type wire coil, the maximum value of the Nusselt number for water shows 304.7 at 70 °C followed by 288.7 at 60 °C and 273.4 at 50 °C, respectively. At 70 °C, using D-type wire coil, the average Nusselt number of the hybrid nanofluid enhances around 11.43% greater than that of the water and 8.05% more than that of hybrid nanofluid at 50 °C, respectively. Using a D-type wire coil, the maximum value of friction factor for water shows 0.2426 at 50 °C followed by 0.2402 at 60 °C and 0.2377 at 70 °C respectively. In contrast, at 50 °C, the average friction factor of the hybrid nanofluid enhances around 13.96% more than that of water and 8.1% more than that of hybrid nanofluid at 70 °C, respectively.

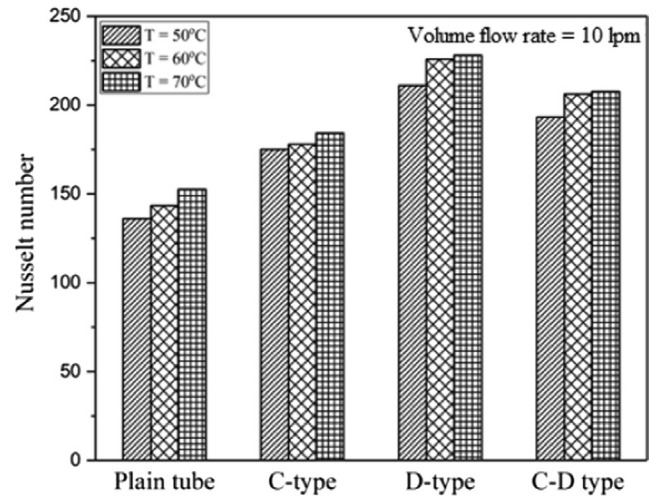


**Fig. 8.** Comparison of Nusselt number for different coil configurations and inlet temperatures.

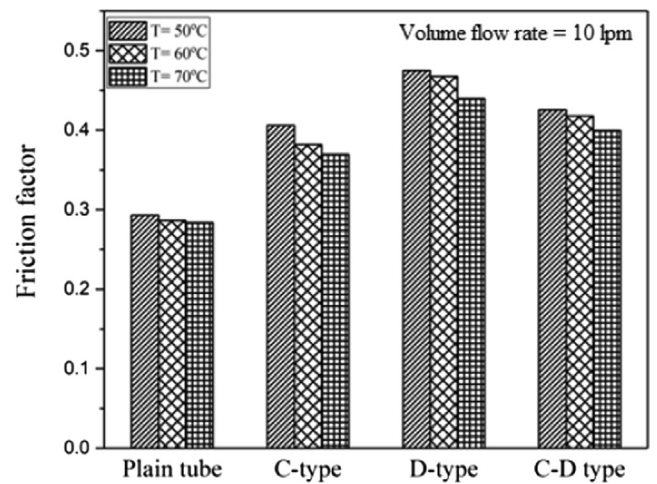


**Fig. 9.** Comparison of friction factor for different coil configurations and inlet temperatures.

### 3.2. Ratio $h/\Delta p$ and thermal performance factor (TPF)

The results obtained so far indicate that using tapered wire coil insertions leads to the augmentation of Nusselt number and reduction of friction factor with the rise in Reynolds number, both of which are favorable. To estimate the net effect of tapered wire coil insertions on the hydrodynamic performance of concentric tube heat exchanger, the ratio  $h/\Delta p$  and TPF have been investigated. **Figs. 10 and 11** show the influence of using tapered wire coil insertions on the  $h/\Delta p$  ratio and TPF of hybrid nanofluid with different configurations (C-type, D-type and C-D type) at the inlet temperature of 60 °C. It has been found that with an increase in Reynolds number, it causes the ratio  $h/\Delta p$  and TPF to diminish up to Reynolds number of 30,000 and then increases. In fact, while increasing the Reynolds number, the pressure drop increases much greater than the heat transfer and this leads to reduce both  $h/\Delta p$  ratio and TPF. The  $h/\Delta p$  ratio varies from 2.92 to 5.05 for the D-type wire coil, 2.72 to 4.85 for the C-D type and 2.71 to 3.88 for the C-type wire coil while using  $Al_2O_3 + MgO$  hybrid nanofluid. In comparison to the  $h/\Delta p$  ratio using nanofluid, D-type wire coil has reported a 5.16% higher than that of water and about 24.9% greater than plane wire coil. The value of TPF is greater than one for hybrid nanofluid. This indicates that using hybrid nanofluid and tapered wire coil insertions are considered a better choice in practical application. In

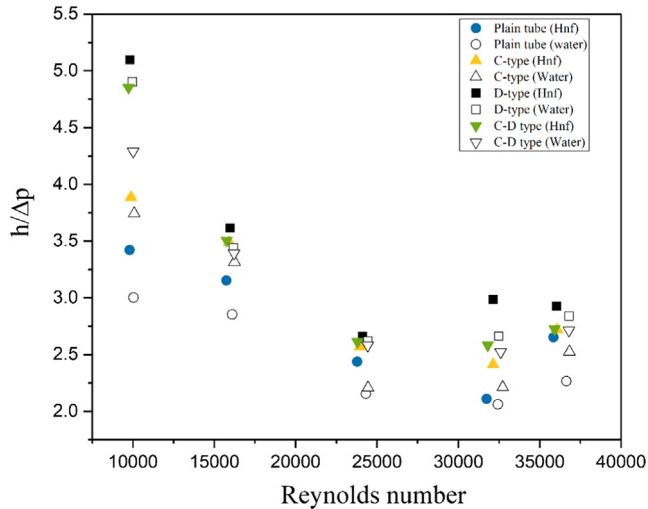


Fig. 10. Variation of  $h/\Delta p$  ratio with Reynolds number for different coil configurations.

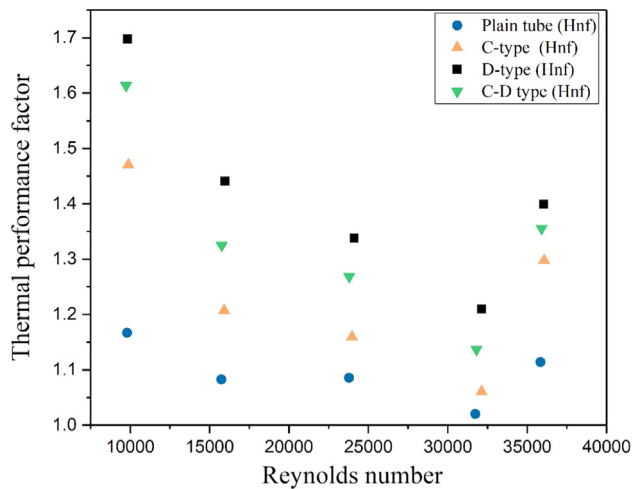


Fig. 11. Variation of TPF with Reynolds number for different coil configurations.

this experimental study, the TPF of nanofluid with D-type wire coil is greater than with C-D type and C-type wire coil inserts. Meanwhile, the maximum TPF of 1.69 was found for the D-type wire coil at Reynolds number of 10000.

Figs. 12 and 13 show the effect of the inlet temperature of hybrid nanofluid on the  $h/\Delta p$  ratio and TPF with different coil configurations at the volume flow rate of 10 lpm. The results reveal that with the rise in hybrid nanofluid inlet temperature, the  $h/\Delta p$  ratio increases but TPF decreases. This is due to the fact that the increase in hybrid nanofluid inlet temperature leads to a reduction of fluid velocity as well as viscosity and thus reduction of the pressure drop. For example, at inlet temperature of 70 °C, using a D-type wire coil, the  $h/\Delta p$  ratio of the hybrid nanofluid enhances by around 20.25% more than that of hybrid nanofluid at 50 °C for the same volume flow rate of 10 lpm. On the other hand, at an inlet temperature of 50 °C, the TPF of the hybrid nanofluid enhances by around 5.35% greater than that of hybrid nanofluid at an inlet temperature of 70 °C.

### 3.3. Entropy generation

Fig. 14 illustrates the variation of total entropy generation with hybrid nanofluid flow rate for different coil configurations at the inlet temperature of 60 °C. As expected, the total entropy genera-

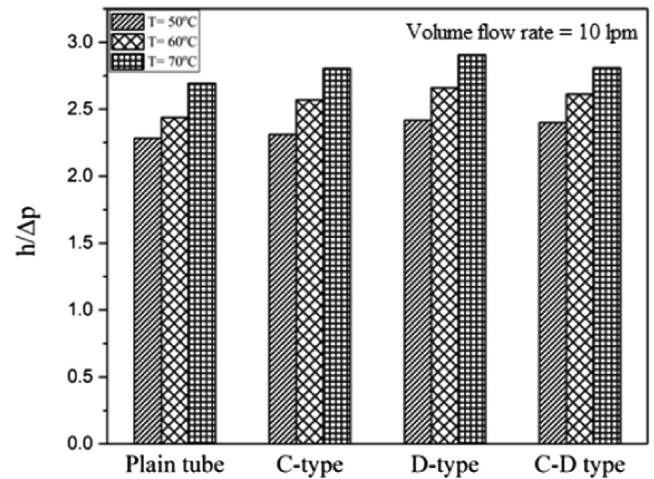


Fig. 12. Comparison of  $h/\Delta p$  ratio for different coil configurations and inlet temperatures.

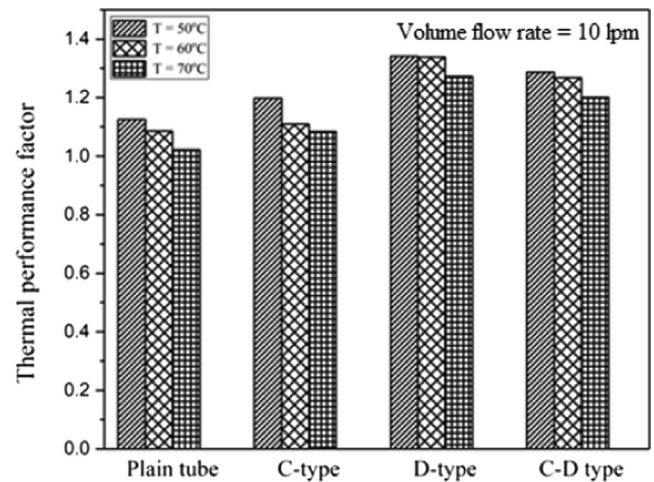


Fig. 13. Comparison of TPF for different coil configurations and inlet temperatures.

tion increases with an increase in the hybrid nanofluid mass flow rate. The entropy generation due to friction ( $S_{gen,f}$ ) is found minor relating to entropy generation due to heat transfer ( $S_{gen,ht}$ ). With the occurrence of nanoparticles in the base fluid, effective temperature difference decreases and pressure drop increases, and as a result,  $S_{gen,ht}$  decreases and  $S_{gen,f}$  increases. As the first part is more significant, the entropy generation of hybrid nanofluid is lower than that of the water. Due to the same reason, the total entropy generation decreases by using tapered wire coil insertions in the tube. In comparison to base fluid, using tapered wire coil insertions in the heat exchanger, the maximum drop in total entropy generation of hybrid nanofluid was found 10.27% for D-type, 6.56% for C-D type and 9.37% for C-type wire coil, respectively, at the Reynolds number of 36000.

Fig. 15 shows the influence of the inlet temperature of the hot fluid (hybrid nanofluid) on the total entropy generation with different wire coil configurations at the volume flow rate of 10 lpm. The result indicates that with the increase in hybrid nanofluid inlet temperature, the total entropy generation increases for all types of wire coil configurations because of the increase in the overall temperature difference of the heat exchanger. It may be known that with an increase in temperature, the fluid properties improve (thermal conductivity increases and viscosity decreases) and hence both heat transfer and friction factor-related entropy generations

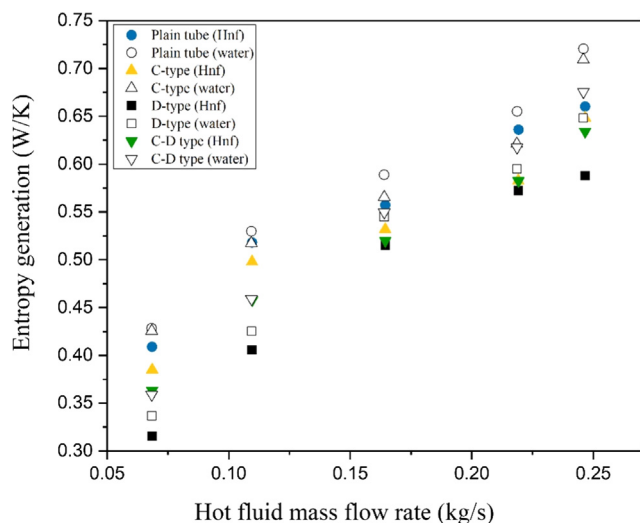


Fig. 14. Variation of entropy generation with hybrid nanofluid mass flow rate for different coil configurations.

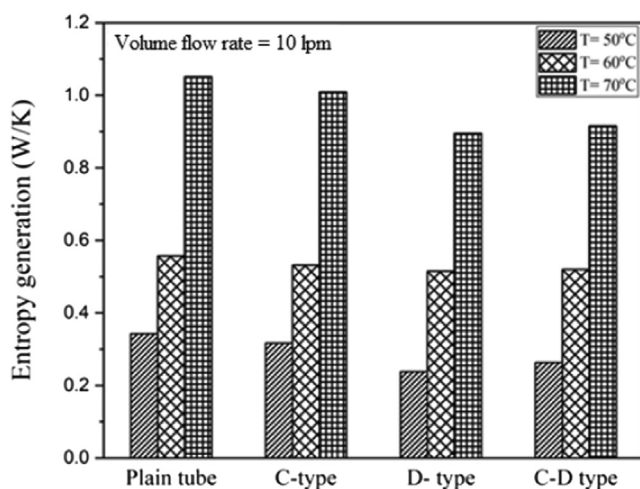


Fig. 15. Comparison of entropy generation for different coil configurations and inlet temperatures.

will decrease for some difference between hot and cold inlet temperatures. At 70°C, the reduction of 17.43% in total entropy generation has been found for D-type wire coil as compared to the smooth tube using hybrid nanofluid.

#### 4. Conclusions

The effects of various types of novel tapered wire coil inserts in the double tube heat exchanger on the heat transfer and friction factor characteristics using  $\text{Al}_2\text{O}_3 + \text{MgO}$  hybrid nanofluid has been studied experimentally under turbulent flow condition. The following conclusions can be obtained from results and discussion:

- D-type wire coil promotes more heat transfer enhancement than others. Nusselt number and friction factor of 0.1% hybrid nanofluid with D-type, C-D type and C-type wire coil inserts enhance 1.64–1.84, 1.57–1.71, 1.34–1.47 times and 1.28–1.68, 1.21–1.57 and 1.18–1.46 times, respectively, as compared to plain tube.

- With the increase in inlet temperature from 50 °C to 70 °C, the Nusselt number of hybrid nanofluid enhances around 8.0% and the friction factor of hybrid nanofluid decreases by 8.1% using D-type wire coil inserts in a double tube heat exchanger.
- The  $h/\Delta p$  ratio using hybrid nanofluid and D-type wire coil insert is about 24.9% more than that of a plane tube using water. The value of TPF is greater than unity for hybrid nanofluid, which indicates that using hybrid nanofluid and tapered wire coil inserts are considered a better choice in practical application
- In comparison to base fluid, using tapered wire coil, the maximum reduction in total entropy generation of hybrid nanofluid is found 10.27% for D-type, 6.56% for C-D type and 9.37% for C-type wire coil, respectively, at Reynolds number of 36000. The total entropy generation of hybrid nanofluid reduces by using wire coil inserts.
- Hybrid nanofluid and tapered wire coil inserts can be considered as a potential combination for improving the hydrothermal characteristics of a double pipe heat exchanger for various heat transfer applications due to an increase in  $h/\Delta p$  ratio.

#### References

- [1] H. Eren, N. Celik, S. Yildiz, A. Durmus, Heat transfer and friction factor of coil-springs inserted in the horizontal concentric tube, *J. Heat Transf.* 132 (2010) 1–11.
- [2] S. Eiamsa-ard, V. Kongkaitpaiboon, P. Promvong, Thermal performance assessment of turbulent tube flow through wire coil turbulators, *Heat Transf. Eng.* 32 (2011) 957–967.
- [3] B.V.N. Ramakumar, J.D. Arsha, P. Tayal, Tapered twisted tape inserts for enhanced heat transfer, *J. Heat Transf.* 138 (2016) 1–9.
- [4] M.E. Nakhchi, J.A. Esfahani, Numerical investigation of turbulent Cu-water nanofluid in heat exchanger tube equipped with perforated conical rings, *Adv. Powder Technol.* 30 (2019) 1338–1347.
- [5] S.K. Singh, J. Sarkar, Improving hydrothermal performance of double-tube heat exchanger with modified twisted tape inserts using hybrid nanofluid, *J. Therm. Anal. Calorimetry* (2020), <https://doi.org/10.1007/s10973-020-09380-w>.
- [6] L. Wang, B. Sundén, Performance comparison of some tube inserts, *International Communications, Heat Mass Transf.* 29 (2002) 45–56.
- [7] K. Ponweiser, W. Linzer, M. Malinovec, Performance comparison between wire coil and twisted tape inserts, *J. Enhanced Heat Transf.* 11 (2004) 359–370.
- [8] N.R. Herring, S.D. Heister, On the use of wire-coil inserts to augment tube heat transfer, *J. Enhanced Heat Transf.* 16 (2009) 19–34.
- [9] A.E. Zohir, M.A. Habib, M.A. Nemitallah, Heat transfer characteristics in a double-pipe heat exchanger equipped with coiled circular wires, *Exp. Heat Transf.* 28 (2015) 531–545.
- [10] D. Panahi, K. Zamzamin, Heat transfer enhancement of shell-and-coiled tube heat exchanger utilizing helical wire turbulator, *Appl. Therm. Eng.* 115 (2017) 607–615.
- [11] S. Khorasani, S. Jafarmadar, S. Pourhedayat, M. Ali, A. Abdollahi, Experimental investigations on the effect of geometrical properties of helical wire turbulators on thermal performance of a helically coiled tube, *Appl. Therm. Eng.* 147 (2019) 983–990.
- [12] C. Pang, J.W. Lee, Y.T. Kang, Review on combined heat and mass transfer characteristics in nanofluids, *Int. J. Therm. Sci.* 136 (2019) 324–354.
- [13] J. Sarkar, P. Ghosh, A. Adil, A review on hybrid nanofluids : Recent research, development and applications, *Renew. Sustain. Energy Rev.* 43 (2015) 164–177.
- [14] V. Kumar, J. Sarkar, Research and development on composite nanofluids as next-generation heat transfer medium, *J. Therm. Anal. Calorimetry* 137 (2019) 1133–1154.
- [15] V. Kumar, J. Sarkar, Experimental hydrothermal characteristics of minichannel heat sink using various types of hybrid nanofluids, *Adv. Powder Technol.* 31 (2) (2020) 621–631.
- [16] S. Rashidi, M. Eskandarian, O. Mahian, S. Poncet, Combination of nanofluid and inserts for heat transfer enhancement: Gaps and challenges, *J. Therm. Anal. Calorimetry* 135 (2019) 437–460.
- [17] M. Chandrasekar, S. Suresh, A.C. Bose, Experimental studies on heat transfer and friction factor characteristics of  $\text{Al}_2\text{O}_3/\text{water}$  nanofluid in a circular pipe under laminar flow with wire coil inserts, *Exp. Therm. Fluid Sci.* 34 (2010) 122–130.
- [18] M. Chandrasekar, S. Suresh, A.C. Bose, Experimental studies on heat transfer and friction factor characteristics of  $\text{Al}_2\text{O}_3/\text{water}$  nanofluid in a circular pipe under transition flow with wire coil inserts, *Heat Transf. Eng.* 32 (2011) 485–496.
- [19] M. Saeedinia, M.A. Akhavan-Behabadi, M. Nasr, Experimental study on heat transfer and pressure drop of nanofluid flow in a horizontal coiled wire inserted tube under constant heat flux, *Exp. Therm. Fluid Sci.* 36 (2012) 158–168.



- [20] M.T. Naik, S.S. Fahad, L.S. Sundar, M.K. Singh, Comparative study on thermal performance of twisted tape and wire coil inserts in turbulent flow using CuO/water nanofluid, *Exp. Therm. Fluid Sci.* 57 (2014) 65–76.
- [21] V.V. Rao, M.C. Reddy, Experimental investigation of heat transfer coefficient and friction factor of ethylene glycol water based TiO<sub>2</sub> nanofluid in double pipe heat exchanger with and without helical coil inserts, *Int. Commun. Heat Mass Transf.* 50 (2014) 68–76.
- [22] M.A. Akhavan-Behabadi, M. Shahidi, M.R. Aligoodarz, An experimental study on heat transfer and pressure drop of MWCNT–water nano-fluid inside horizontal coiled wire inserted tube, *Int. Commun. Heat Mass Transf.* 63 (2015) 62–72.
- [23] M.A. Akhavan-Behabadi, M. Shahidi, M.R. Aligoodarz, M. Ghazvini, Experimental investigation on thermo-physical properties and overall performance of MWCNT–water nanofluid flow inside horizontal coiled wire inserted tubes, *Heat Mass Transf.* 53 (2017) 291–304.
- [24] M. Mirzaei, A. Azimi, Heat transfer and pressure drop characteristics of graphene oxide/water nanofluid in a circular tube fitted with wire coil insert, *Exp. Heat Transf.* 29 (2016) 173–187.
- [25] K. Goudarzi, H. Jamali, Heat transfer enhancement of Al<sub>2</sub>O<sub>3</sub>-EG nanofluid in a car radiator with wire coil inserts, *Appl. Therm. Eng.* 118 (2017) 510–517.
- [26] L.S. Sundar, P. Bhramara, N.T.R. Kumar, M.K. Singh, A.C.M. Sousa, Experimental heat transfer, friction factor and effectiveness analysis of Fe<sub>3</sub>O<sub>4</sub> nanofluid flow in a horizontal plain tube with return bend and wire coil inserts, *Int. J. Heat Mass Transf.* 109 (2017) 440–453.
- [27] E.F. Akyurek, K. Gelis, B. Sahin, E. Manay, Experimental analysis for heat transfer of nanofluid with wire coil turbulators in a concentric tube heat exchanger, *Results Phys.* 9 (2018) 376–389.
- [28] K.A. Hamid, W.H. Azmi, R. Mamat, K.V. Sharma, Numerical investigation for turbulent heat transfer of TiO<sub>2</sub>-SiO<sub>2</sub> nanofluids with wire coil inserts, *Numer. Heat Transf. A: Appl.* 75 (2019) 271–289.
- [29] K.A. Hamid, W.H. Azmi, R. Mamat, K.V. Sharma, Heat transfer performance of TiO<sub>2</sub>-SiO<sub>2</sub> nanofluids in a tube with wire coil inserts, *Appl. Therm. Eng.* 152 (2019) 275–286.
- [30] H. Karakaya, A. Durmus, Heat transfer and exergy loss in conical spring turbulators, *Int. J. Heat Mass Transf.* 60 (2013) 756–762.